Abdominal Radiology

Published online: 26 May 2018

Abdom Radiol (2019) 44:1999–2008
https://doi.org/10.1007/s00261-018-1649-2

Texture analysis of small renal cell carcinomas at MDCT for predicting relevant histologic and protein biomarkers

Andrew T. Scrima,[1] Meghan G. Lubner,[1] E. Jason Abel,[2] Thomas C. Havighurst,[3] Daniel D. Shapiro,[2] Wei Huang,[4] and Perry J. Pickhardt[1]

[1]Department of Radiology, University of Wisconsin School of Medicine and Public Health, E3/311 Clinical Sciences Center, 600 Highland Ave, Madison, WI 53792, USA
[2]Department of Urology, University of Wisconsin School of Medicine and Public Health, Madison, USA
[3]Department of Biostatistics, University of Wisconsin School of Medicine and Public Health, Madison, USA
[4]Department of Pathology, University of Wisconsin School of Medicine and Public Health, Madison, USA

Abstract

Purpose: To assess CT texture features of small renal cell carcinomas (≤ 4cm) for association with key pathologic features including protein biomarkers.
Methods: Quantitative CT texture analysis (CTTA) of small renal cancers (≤ 4cm) was performed on non-contrast and portal venous phase abdominal MDCT scans with an ROI drawn at the largest cross-sectional diameter of the tumor using commercially available software. Texture parameters including mean pixel attenuation, the standard deviation (SD) of the pixel distribution histogram, entropy, the mean of positive pixels, the skewness (i.e., asymmetry) of the pixel histogram, kurtosis (i.e., peakness) of the pixel histogram, and the percentage of positive pixels were correlated with pathologic data from surgical resection, including histology and nuclear grade, as well as microarray analysis in a subset ($n = 40$) including Ki67 index, CRP, and neovascularization (CD105/CD31).
Results: Portal venous phase images were available in 249 patients (105 women, 144 men; mean age, 56.7 years) with tumors ≤ 4cm (mean, median, range, ± SD; 2.66, 2.60, 0.3–4.0 ± 0.85 cm). CT texture features of standard deviation, mean of the positive pixels, and entropy of the pixel histogram were significantly associated with histologic cell type (clear vs. non-clear; $p < 0.001$). Entropy and mean of the positive pixels also showed an association with nuclear grade, although not statistically significant. In the microarray analysis subset, kurtosis of the pixel histogram was associated with CD105/CD31 ($p = 0.05$). SD also showed some association with CD 105 positivity ($p = 0.02$) and CAIX expression ($p = 0.01$). Non-contrast CT images were available in 174 patients (72 women, 102 men; mean age, 57.5 years). Although the association with histology was not as strong as on the portal venous phase, in the subset of patients with microarray data, SD was found to correlate with CRP ($p = 0.08$), kurtosis with CRP ($p = 0.004$), CD105/CD31 ($p = 0.002$), and with Ki 67 index ($p < 0.001$).
Conclusion: CT texture features were significantly associated with important histopathologic features in small renal cancers. These non-invasive measures can be performed retrospectively and may provide useful information when determining follow-up and treatment of small renal cancers.

Key words: Small renal mass—CT—CT texture analysis—Protein expression

Renal cell carcinoma (RCC) is the third most common urologic malignancy and accounts for 2–3% of malignant disease in adults. Small renal cell tumor masses frequently have a more favorable prognosis (i.e., lower nuclear grade, decreased mortality) compared to larger masses [1]. However, it is known that a subset of small renal tumors demonstrate more aggressive behavior including early metastatic spread, high tumor grade, and advanced pathologic stage, and size alone is not sufficient to distinguish more aggressive pathologic features [2, 3]. Therefore, these patients would benefit from

Correspondence to: Meghan G. Lubner; *email:* mlubner@uwhealth.org

additional data to aid in identifying more aggressive tumors, which could lead to improved risk stratification and more informed clinical decision making.

Various studies have shown CT and MRI can identify potential useful imaging biomarkers including diffusion restriction, apparent diffusion coefficient values, and features of dynamic contrast enhancement [4–11]. Another potentially useful emerging biomarker is CT tumor texture analysis. Textural analysis provides a gross assessment of heterogeneity by analyzing the distribution and association with pixel or voxel gray level in the image [12, 13]. It has shown promise in predicting pathologic features, overall survival, and response to therapy for a variety of tumor types [14–19]. In addition, texture analysis can be performed retrospectively on CT scans performed for other purposes where a renal mass may be incidentally detected [20].

Raman et al. [21] showed that texture features can be used to reliably discriminate between different types of renal masses (e.g., clear cell RCC papillary RCC, oncocytoma, and benign renal cysts). Goh et al. [22] found tumor texture could also be used to assess RCC treatment response after treatment with tyrosine kinase inhibitors. More recently, CT textural features of larger renal masses (> 7 cm) showed association with histologic subtype, nuclear grade, and clinical outcomes [23]. However, to our knowledge, there are limited published data that assess the value of texture analysis for untreated primary small renal cell carcinoma where this type of data could be very useful for clinical decision making. The purpose of this study is to determine whether the CT texture features of small primary RCCs (≤ 4 cm) are associated with pathologic tumor features including histologic subtype, protein biomarkers, and clinical outcomes.

Methods and materials

The study was approved by the institutional review board at the University of Wisconsin School of Medicine and Public Health and was HIPAA compliant.

Patient population

The non-contrast CT images of 174 patients (72 women and 102 men; mean age, 57.5 years) and portal venous CT images of 249 patients (105 women and 144 men; mean age 56.7 years) with small (≤ 4 cm) Patients from a surgical database of the Department of Urology were retrospectively reviewed. Inclusion criteria included patients with small RCC (≤ 4 cm) with pathologic analysis and CT scan prior to surgery with unenhanced or portal venous images. Exclusion criteria included large RCC (> 4 cm), no pathologic analysis, no unenhanced or portal venous images and the presence of sarcomatoid features, rhabdoid features, or metastases due to a small subset of patients with these features. Patients had a CT scan performed prior to surgery (mean = 81 days). Standard pathologic analysis from surgical resection included histology and nuclear grade. Additional microarray analysis was available for a subset of patients (33 patients with non-contrast images and 40 with portal venous CT images) where additional pathologic markers were evaluated [24]. Clinical and imaging follow-up data were also obtained for all patients from the PACS and the electronic medical records. Patient status (i.e., no evidence of disease, alive with disease, deceased due to disease, or deceased due to other causes) at the time of the last clinical or imaging follow-up examination was also obtained

CT images and analysis

Examinations were classified based on the contrast phase used. For each phase of contrast, measurements were made and CT texture findings were recorded. Images and data were compared from the same contrast phase only. The two largest series of images were obtained in the unenhanced images and portal venous or nephrographic phase images so images obtained in these phases were the focus of the analysis. Prior work showed that the non-contrast and portal venous phases were the highest yield when evaluated for associations with renal pathology [23]. For this reason, and due to small subset of patients with arterial phase imaging (n = 53) and microarray analysis (n = 10), the arterial phase was not included in the study. CT scans were performed using MDCT scanners, and the imaging parameters were as follows: a tube potential of 100–140 kV (with most of the scans using a tube potential of 120 kV) and a matrix of 512 × 512 × 16. Most scans were performed using automated or variable tube mA, and the slice thickness used was 2–5 mm. It has been shown that this method of texture measurement is relatively resistant to differences in technique [25].

A single slice at the level of the overall largest transverse diameter of the tumor was selected by a single reader, a medical student who was under the supervision of the two abdominal imaging radiologists (MGL with 9 years of experience, PJP 20 years of experience). These single-slice images were transferred to a commercially available texture analysis software program (TexRAD Ltd, part of Feedback Plc, Cambridge, UK) allowing an ROI to be manually drawn around the outer margin of the tumor by the same reader. The software uses an initial filtration step and a Laplacian of gaussian spatial bandpass filter to selectively extract features of different sizes and variations in intensity [22, 26]. This allows features to be examined with texture filter settings ranging from fine (spatial scaling factor, 2; width, ≈ 4 pixels; object radius, ≈ 2 mm) to coarse (spatial scaling factor, 5–6; width, ≈ 12 pixels; object radius, ≈ 6 mm)

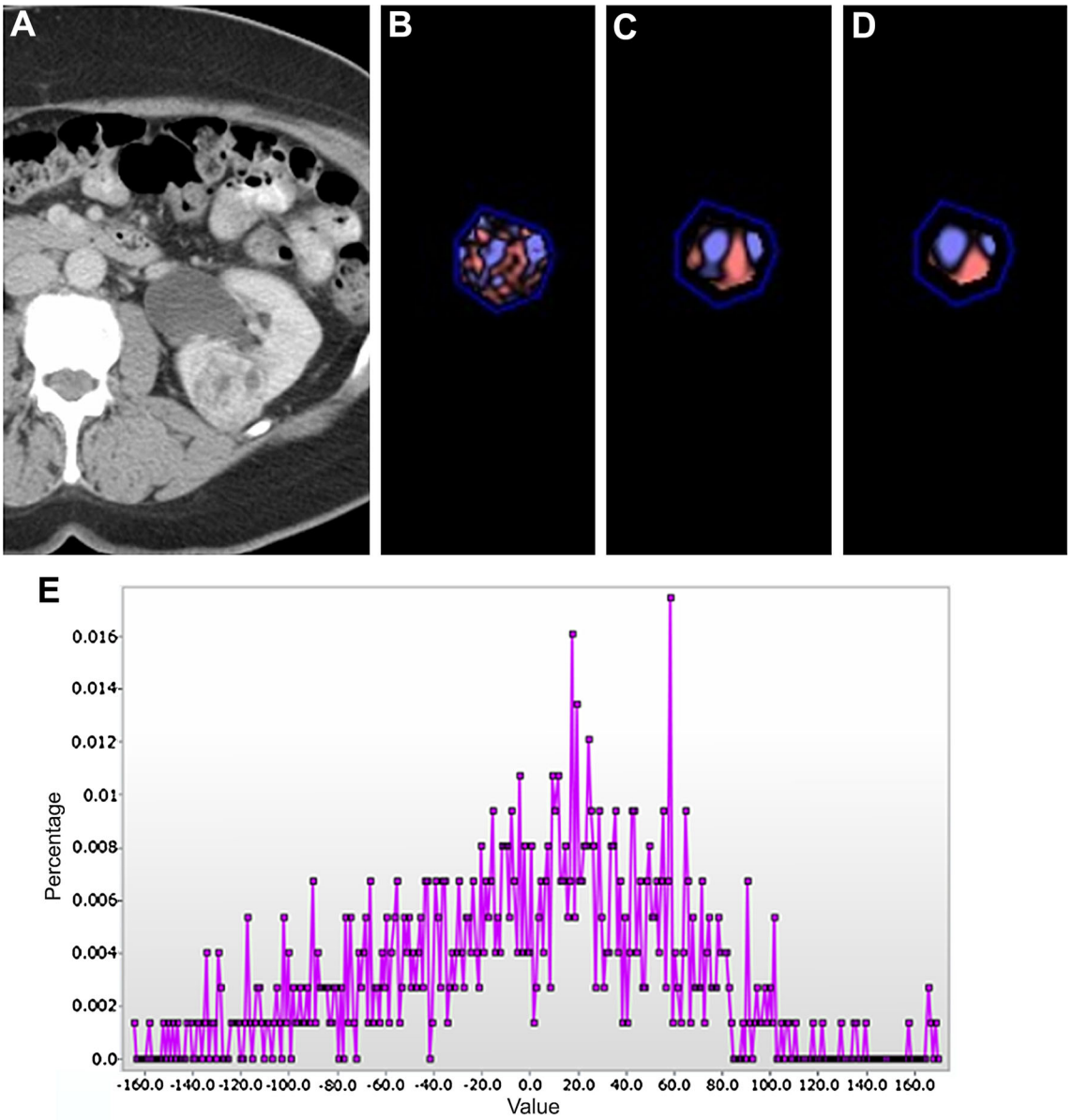

Fig. 1. CT texture analysis of clear cell vs. papillary renal cell carcinoma. A heterogeneous lesion is seen in the posterior aspect of the left kidney on CECT (**A**). CT texture maps at fine (**B**), medium (**C**), and coarse (**D**) spatial scaling factors show positive pixels in pink or red and negative pixels in blue or purple. A pixel histogram (**E**) is created (ssf 2, fine features shown), which demonstrated a range of pixel attenuations and how often they occur. Note that the overall values are more heterogeneous and higher in attenuation than those seen in a papillary renal cell carcinoma (CECT **F**, texture maps **G–I**, pixel histogram, **J**).

[25, 27]. The software output includes a variety of histogram characteristics, including mean pixel attenuation, the standard deviation (SD) of the pixel distribution histogram, entropy, the mean of positive pixels, the skewness (i.e., asymmetry) of the pixel histogram, kurtosis (i.e., peakness) of the pixel histogram, and the percentage of positive pixels for each spatial scaling factor (Fig. 1). These values were recorded and analyzed based on contrast phase (with data from each contrast phase evaluated separately). Texture features were analyzed against histologic subtype, nuclear grade, presence of metastatic disease, time to disease recurrence, and time to death from disease. Nuclear grade was not applied to chromophobe RCCs, so such RCCs are categorized as having an unknown grade. An assessment of texture features in identifying aggressive tumors as defined by greater than stage T3a or nuclear grade 3–4 was also performed. Additional microarray analysis included Ki-67 mean OD, Ki-67 index, CD 105:CD 31 ratio (neovascularity), CD 31 mean OD, CD 105 mean OD, CD 105 positivity, MSKCC 5 year% recurrence, carbonic anhydrase IX (CAIX) cytoplasm mean OD, CAIX nu-

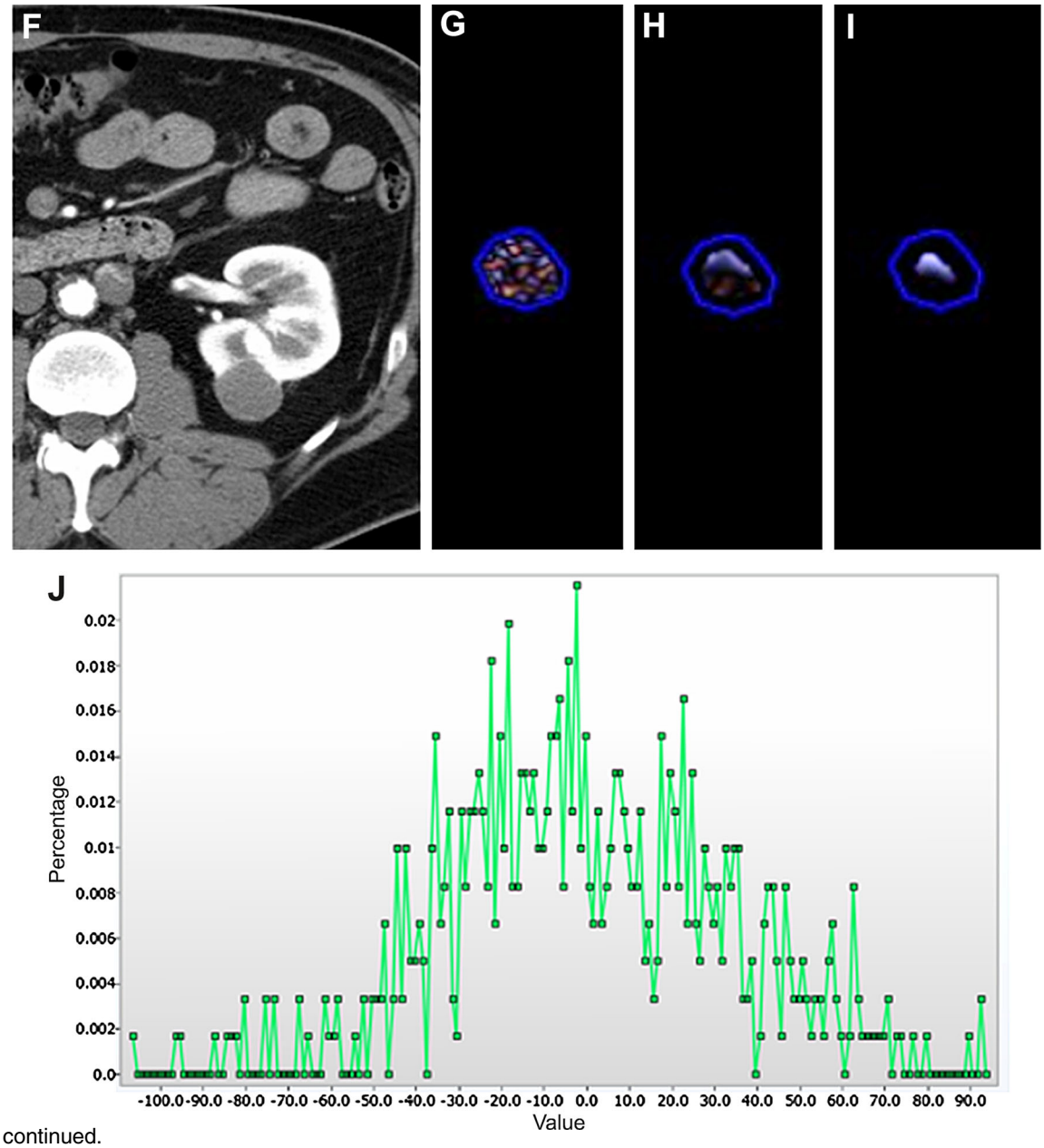

Fig. 1. continued.

cleus mean OD, C-reactive protein (CRP) cytoplasm nucleus OD, CRP nucleus mean OD, total CRP, Hypoxia-inducible factors (Hif) 1a N:C ratio, Hif2a N:C ratio, total Hif1a, and total Hif2a (Fig. 2). Protein biomarkers were selected by Department of Urology in collaboration with pathology GU-trained pathologist[24].

Statistical analysis

Frequencies were calculated for categorical variables and descriptive statistics for continuous variables. Various methods were utilized to assess the relationship between CT texture features and clinical data or outcomes. Ordinal logistic regression was used to analyze ordinal categorical variables (nuclear grade). Logistic regression for binary variables (RCC subtype), and general linear models were used for continuous variables (Ki-67 index). Survival data were analyzed with Cox proportional hazards regression. The six texture features were assessed at each filter level and for each contrast phase (i.e., the unenhanced phase, and portal venous phase). A Bonferroni correction was applied to account for the filter-level multiple comparisons. Normality plots were done and SD was converted to logarithmic scale to improve normality. Examinations of categorical variables are displayed using box plots and continuous variables with

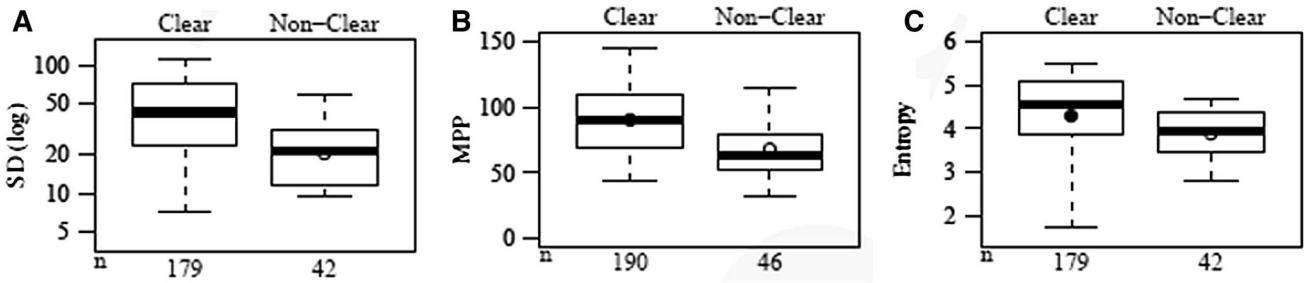

Fig. 2. Texture features in clear vs. non-clear cell renal cell carcinoma. **A** Box and whisker plot comparing SD (**A**) of pixel distribution histogram and RCC subtype at coarse feature size (ssf 6). SD is positively associated with clear cell vs. non-clear cell subtype on portal venous imaging. Similarly, mpp on portal venous phase is also positively associated with clear cell subtype (**B**, ssf 0). Entropy on portal venous phase imaging is also higher in clear cell tumors than non-clear cell (**C**, ssf 6).

Table 1. Demographic and clinical characteristics of patients with renal cell carcinoma

Characteristic	All patients	Patients with portal venous or nephrographic phase images (n = 249)	Patients with unenhanced images (n = 174)	Patients with both unenhanced and portal venous images (n = 148)	Patients with microarray analysis (n = 41)
Age (years), mean	57.2	56.7	57.5	56.8	62.8
No. of patients	273	249	174	148	41
Female	115	105	72	59	16
Male	158	144	102	89	25
Tumor diameter (cm)					
Mean ± SD	2.66 (0.85)	2.65 (0.86)	2.60 (0.86)	2.58 (0.85)	2.71 (0.92)
Median	2.60	2.55	2.50	2.50	2.60
Range	0.3–4.0	0.3–4.0	0.3–4.0	0.3–4.0	0.3–4.0
Tumor histologic subtype					
Clear cell	214	196	134	112	31
Papillary	38	32	26	22	8
Chromophobe	10	10	7	7	1
Unclassified	11	11	7	7	1
Nuclear grade					
1	60	57	38	33	19
2	149	137	96	85	16
3	39	32	23	17	1
4	7	6	4	2	2
Unknown	18	17	13	11	3
Sarcomatoid features, no. (%) of patients	2 (0.7)	2 (0.8)	2 (1.2)	1 (0.7)	0 (0)
Metastatic disease present at surgery, no. (%) of patients	3 (1.1)	3 (1.2)	1 (0.6)	2 (1.3)	1 (2.4)
Clinical follow-up duration (mo)					
Mean ± SD	44.5 (38.9)	43.9 (38.6)	45.0 (40.3)	45.5 (41.8)	68.5 (53.6)
Median	30.6	30.8	30.4	31.3	62.3
Range	0.1–166.4	0.1–166.4	0.1–166.4	0.1–166.4	0.4–159.3
Patient status					
Deceased	41	37	23	19	18
Renal cell carcinoma related	12	11	7	6	4
Unknown or alternate cause	29	26	16	8	14
Alive	232	211	151	129	23
With no evidence of disease	226	205	147	125	20
With disease	6	6	4	4	3

scatter plots. Kaplan–Meier survival estimates were constructed and displayed for each group. Multiple masses from the same patient were treated as independent masses.

Results

Demographic and clinical features for the cohort are displayed in Table 1. All tumors analyzed were ≤ 4 cm

Table 2. CT textural features association with histologic subtype

	Histologic subtype	*p* value
Portal venous CT texture feature		
SD of pixel histogram	Clear cell vs. non-clear cell	0.007 (ssf 0); < 0.001 (ssf 2, 3, 4, 5, 6)
Mean of positive pixels	Clear cell vs. non-clear cell	< 0.001 (ssf 0, 2, 3, 4, 5); 0.002 (ssf 6)
Entropy	Clear cell vs. non-clear cell	0.005 (ssf 0,2); 0.009 (ssf 3); 0.014 (ssf 4); 0.011 (ssf 5)
Non-contrast CT texture feature		
Mean gray-level intensity	Clear cell vs. non-clear cell	0.046 (ssf 5); 0.030 (ssf 6)

Table 3. CT textural features association with microarray analysis

	Tumor microarray	*p* value
Portal Venous CT texture feature		
SD of pixel histogram	CD 105 positivity	0.018 (ssf 4); 0.015 (ssf 5, 6)
Entropy	CD 105 positivity	0.05 (ssf 2); 0.036 (ssf 3)
SD of pixel histogram	CAIX cytoplasmic mean	0.036 (ssf 2); 0.008 (ssf 3); 0.029 (ssf 4)
SD of pixel histogram	CAIX nuclear mean	0.012 (ssf 2); 0.004 (ssf 3); 0.014 (ssf 5)
Kurtosis	CD 105/CD 31	0.05 (ssf 6)
Non-contrast CT texture feature		
Kurtosis	Ki-67 index	< 0.001 (ssf 0)
Kurtosis	CD 105/CD 31	0.002 (ssf 2)
Kurtosis	CRP nuclear mean	0.004 (ssf 0)
Kurtosis	CRP cytoplasmic mean	0.042 (ssf 0)
Kurtosis	Total CRP	0.037 (ssf 0)
Kurtosis	HiF2a nuclear: cytoplasmic ratio	0.015 (ssf 0)
Entropy	HiF2a N:C	0.017 (ssf 0)
SD of pixel histogram	HiF2a N:C	0.003 (ssf 0); 0.039 (ssf 2)
Mean positive pixel	HiF2a N:C	0.022 (ssf 2); 0.038 (ssf 3)

(mean, median, range ± SD; 2.66, 2.60, 0.3–4.0 ± 0.85 cm). The majority of tumors were clear cell histologic subtype (n = 214/78.3%), with some papillary and chromophobe subtypes noted. Nuclear grades were obtained for the tumors (papillary and clear cell subtypes) and the majority were assigned a nuclear grade of 2 or lower (Table 1). Nuclear grade was not assigned to chromophobe tumors (2.7%). Outcome variables sarcomatoid features (n = 2), rhabdoid features (n = 0), and metastases (n = 3) were excluded from our analysis, as the incidence was too small to test any differences.

The mean duration of clinical follow-up after resection was 44.5 months (median 30.6, range 0.1–166.4 months). At the time of last follow-up, 37 patients (14.9%) with portal venous imaging and 21 (13.2%) with unenhanced imaging were deceased. Of the deceased patients, 11 (29.7%) and 7 (30.4%), respectively, were RCC related, whereas the others were due to reasons unrelated to RCC. For those alive at the last follow-up, 206 patients (97.2%) with portal venous imaging and 147 (97.4%) with unenhanced imaging had no evidence of disease, while 6 and 4 patients, respectively, were alive with disease.

CT texture features on portal venous phase images that showed the strongest association with histologic findings were SD of pixel distribution histogram and mean of the positive pixels (mpp). Both were positively associated with clear cell subtype for all filter levels (Table 2). For example, when images were obtained with a spatial scaling factor of 6 (coarse or large feature size), the mean SD of the pixel distribution histogram value for clear cell subtype was 4.58 (SD = 0.28) vs. 4.42 (SD = 0.24) for non-clear cell subtypes ($p < 0.001$) (Fig. 2A). Mean of the positive pixels (mpp) was also found to be positively associated with clear cell subtype (ssf 2; m = 49.60, SD = 23.29) vs. non-clear cell subtype (m = 32.46, SD = 24.07) which was most prominent at finer filter settings, but again, persisted for all filter settings (Fig. 2B). Entropy also showed positive association with clear cell subtype which was most pronounced with finer filter settings (Table 2). For example, when images were obtained with a spatial scaling factor of 2, mean entropy value for clear cell subtype was 4.89 (SD = 0.89) vs. 4.52 (SD = 0.45) for non-clear cell subtype (p = 0.005) (Fig. 2C). Surprisingly, entropy was not associated with histologic subtype when images were obtained with coarse filter texture setting, unlike previous investigation into textural analysis of larger renal cell carcinoma, possibly related to the smaller size of these lesions.

On non-contrast images, one texture feature was associated with renal cell carcinoma subtype (Table 2). Mean gray-level intensity was negatively associated with clear cell carcinoma on coarse filter settings. For example, with a spatial scaling factor of 5, the mean value for mean gray-level intensity was 2.72 (SD = 12.52) for clear cell subtype vs. 10.28 (SD = 14.42) for non-clear

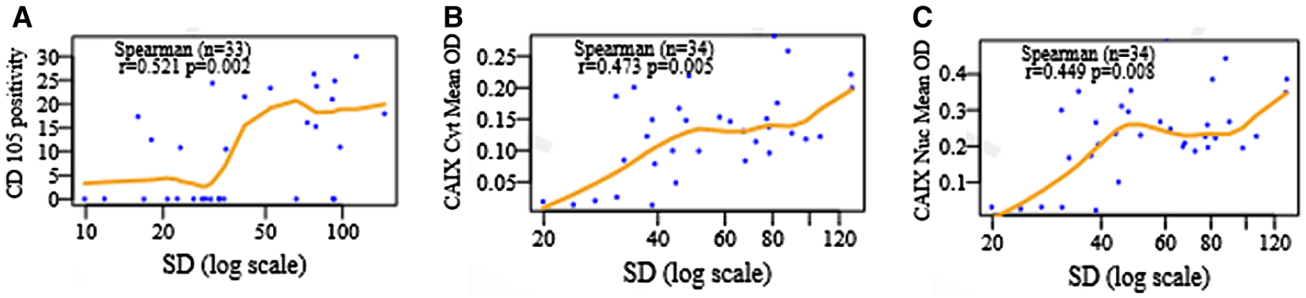

Fig. 3. Scatter plots comparing SD and protein biomarkers. SD is positively associated with CD 105 positivity on portal venous imaging (**A**, ssf 6). Similar positive associations are seen between SD and CAIX cytoplasmic mean (**B**, ssf 3) and CAIX nuclear mean (**C**, ssf 3) also on portal venous imaging.

cell subtype ($p = 0.046$), and with spatial scaling factor of 6, the mean value for mean gray-level intensity was 17.13 (SD = 4.40) for clear cell subtype vs. 17.40 (SD = 3.44) for non-clear cell subtype ($p = 0.030$). There was also trending negative association between skewness and nuclear grade but only when images were obtained with coarse filter settings (ssf 5; $p = 0.076$). There was no relationship between textural features and aggressive features (> stage T3a or nuclear grade 3–4) or survival outcomes regardless of contrast phase.

In the subset of patients who had tissue evaluated in tumor microarray (Table 1), there were several significant associations between textural features and protein expression (Table 3). On portal venous imaging, SD of pixel distribution histogram and entropy were associated with CD 105 positivity. The strongest association between SD and CD 105 positivity was present when images were obtained with coarse filter settings (ssf 5–6; $p = 0.015$) but not present with finer filter settings (Fig. 3A). Entropy was associated with CD 105 when images were obtained with fine and medium texture settings (ssf 2; $p = 0.036$ & ssf 3; $p = 0.05$) but not with coarse filter settings. SD of pixel histogram distribution was also correlated with CAIX cytoplasmic and nuclear mean on fine and medium settings. For example, when images were obtained with spatial scaling factor of 3, SD of pixel histogram distribution was positively associated with CAIX cytoplasmic mean ($p = 0.008$) and nuclear mean ($p = 0.004$) (Fig. 3B, C). Additionally, kurtosis of pixel histogram was associated with CD105/CD31 at coarse filter settings (ssf 6; $p = 0.05$).

On non-contrast imaging, there were also several relationships between textural features and protein expression, many of which were most prominent at fine or unfiltered settings (Table 3). The strongest association was between kurtosis of pixel histogram and Ki-67 index with unfiltered settings (ssf 0; $p < 0.001$). Kurtosis was also positively associated with several other protein biomarkers on fine or unfiltered settings including CD 105/31 (ssf 2; $p = 0.002$), CRP nuclear mean (ssf 0; $p = 0.004$), total CRP (ssf 0; $p = 0.037$), and CRP cytoplasmic mean (ssf 0; $p = 0.042$). On the other hand, kurtosis demonstrated negative association with HiF2a nuclear: cytoplasmic ratio on unfiltered setting ($p = 0.015$). Several other textural variables were found to have positive association with Hif2a N:C ratio on fine and unfiltered settings including entropy (ssf 0; $p = 0.017$), SD (ssf 0; $p = 0.003$, ssf 2; $p = 0.039$) and mean positive pixels (ssf 2; $p = 0.022$ & ssf 3; $p = 0.038$). In addition, there were some textural features that were trending toward associations but did not reach statistical significance including positive relationship between skewness of pixel histogram and Ki-67 nuclear mean (ssf 6; $p = 0.066$), SD and HiF1a N:C ratio (ssf 0; $p = 0.071$) and negative association between skewness and Ki-67 index (ssf 0; $p = 0.076$), and SD and CAIX cytoplasmic mean (ssf 5; $p = 0.068$).

Discussion

The incidence of RCC in the US has steadily increased coinciding with a decrease in the size of renal masses, partly due to increased detection of incidental small renal cell tumors [28–30]. Despite a higher proportion of smaller, early-stage RCC, the RCC-related mortality has also continued to increase due to a subset of small RCC which demonstrate aggressive features such as early metastasis, high tumor grade, or advanced pathologic stage [1–3, 19]. CT and MRI are frequently used for clinical staging of RCC prior to treatment but there remains a need for additional prognostic information to better distinguish these aggressive features to allow more accurate risk stratification and appropriate treatment selection. Several imaging biomarkers have been reported using contrast-enhanced CT and MRI, but prior studies have not investigated the use of textural analysis for patients with small RCC before surgery.

Heterogeneity is a well-recognized feature of malignancy and can represent adverse tumor biology [31]. Heterogeneity is thought to reflect a tumor's microenvironment including differences in genomics, cellularity, growth, angiogenesis, and metabolism [32]. Texture analysis is an image processing algorithm that can be used to detect and quantify this heterogeneity and to

identify textural irregularities not easily visible to naked eye. Researchers have demonstrated associations between CT texture and histopathologic features and genetic profiles for multiple types of tumors as well as correlations with clinical outcomes such as survival and response to treatment [14–18, 21–23].

In patients with RCC, Raman et al. [21] and Hodgdon et al. [33] demonstrated that CT texture analysis can distinguish between benign and malignant renal lesions as well as between some malignant histologic subtypes. Another group examined CT textural features for large RCC (> 7 cm) and found textural features including entropy, SD of pixel distribution histogram, and mean of the positive pixels to be associated with tumor histologic subtype, nuclear grade, and clinical outcomes [23]. However, there is a lack of data examining the ability of CT textural analysis to provide similar prognostic information for untreated small RCCs which can provide more of a challenge when facing treatment decisions. We found pretreatment CT textural analysis can provide important supplemental information regarding characterization of histologic subtype and provide further insight into a tumor's microenvironment such as tissue biomarkers and protein expression.

When texture findings were compared to standard surgical pathological analysis, we found SD of pixel histogram, mean of the positive pixels, and entropy were each associated with RCC histologic subtype on portal venous imaging. These texture features maintained statistical significance across several filter settings, increasing our confidence that these represent true relationships and less likely to be confounded by noise. Entropy, a measure of texture irregularity, and SD of pixel histogram distribution represent increased tumor heterogeneity and these findings suggest there may be more heterogeneity seen with clear cell subtype vs. non-clear cell subtypes. SD of pixel histogram has previously been shown to be positively associated with hypoxia in non-small cell lung cancer and negatively associated with angiogenesis in colorectal cancer [34]. Hypoxia and decreased angiogenesis is typically associated with necrosis which could explain the greater variability and heterogeneity captured on contrast-enhanced imaging. Mean of positive pixels also was positively associated with clear cell subtype, possibly in association with enhancement or hemorrhage. Our findings showed similar relationships between SD of pixel histogram, mean of the positive pixels, and RCC subtype compared to studies done in larger RCCs. However, entropy was not associated with histologic subtype on coarse filter settings as seen with large RCC (this relationship was only seen at smaller feature sizes in small RCC). This could represent increased microscopic heterogeneity in smaller renal masses compared to more macroscopic areas with larger masses. Mean gray-level intensity was positively associated with clear cell subtype at more coarse filter settings only and was the only unenhanced texture feature to reach statistical significance for predicting RCC subtype. Collectively, these data suggest that unenhanced CT texture features may not be as useful for discerning renal cell subtypes in small renal masses.

We were unable to identify any associations between textural features and nuclear grade for either contrast-enhanced or unenhanced imaging. However, we observed trends toward a negative association between entropy and nuclear grade and positive association between mean of the positive pixels and nuclear grade which were similar to those observed in large RCC cohort, although these did not reach statistical significance. Similarly, we did not find any specific texture feature that predicted aggressive tumor behavior as defined by stage greater than T3a or nuclear grade 3–4. However, the relatively small number of tumors with higher nuclear grades or aggressive features may limit our ability to identify meaningful associations. Unlike previous studies investigating textural analysis in larger RCC, we did not identify a relationship between renal mass texture features and survival outcomes. Similar to the evaluation of grade and stage, the small percentage of small RCC population who died from their disease (4.4% cancer mortality) likely limits the ability to evaluate survival outcomes unlike the population with larger RCC (36% cancer mortality). Both of these areas warrant further investigation in larger cohorts of small renal masses as associations between CT texture features and aggressive tumor features or clinical outcomes could be very useful in prognostication and triage for treatment type or potentially observation of small renal masses.

Despite the lack of significant association with aggressive pathologic features as defined by nuclear grade and tumor stage, in the subset of patients who underwent additional microarray pathologic analysis, several textural features were associated with the presence of tissue protein expression which could also be useful in determining tumor biology and behavior. Certain putative biomarkers including Ki-67 positivity, CRP, CAIX, and HiF expression have been used to successfully differentiate malignant vs. benign renal tissue and shown to have prognostic value in certain cases [24, 35]. HIF tends to accumulate in hypoxic environments or with VHL deficiency and has been associated with clear cell RCC vs. non-clear cell subtype; however, the prognostic value remains controversial [36–38]. Ki-67 is a cellular marker for cellular proliferation and has been associated with nuclear grade, poor clinical outcomes, and RCC recurrence [39, 40]. CD 105 positivity and CAIX expression appear to play roles in tumor angiogenesis and hypoxic response, respectively, and have both been shown to be inversely associated with prognosis in RCC [41, 42]. CD 105/CD31 represents neovascularization and has been associated with increasing nuclear grade and poorer overall survival [43].

P53 positivity is a well-studied oncologic marker but appears to be less common in RCC, especially clear cell subtype [44]. On portal venous imaging, we found both entropy and SD of pixel histogram were positively associated with CD 105 positivity across multiple filter settings, suggesting these features may in some way be related to neovascularity. Moreover, SD was positively associated with both CAIX cytoplasmic mean and nuclear mean across multiple filter settings, while mean of the positive pixels also showed a positive association with CAIX cytoplasmic mean on unfiltered setting and several other filter settings trending toward significance for both CAIX measures. Kurtosis was also found to be correlated with Ki-67 index, CD 105/35, and CRP nuclear mean, cytoplasmic mean, and total CRP. There were other textural features whose relationship with tissue biomarkers or protein expression reached significance; however, these only occurred with single filter settings. Although these data are very promising, only a small subset of patients underwent microarray analysis so additional investigation with larger sample size is necessary. Further, direct correlation between pathology and the exact site being imaged needs to be performed.

It is hard to predict where CT texture analysis could fit in our current clinical algorithm for assessing small renal masses. As noted, a large number of patients undergo routine CT for indications other than evaluation of renal masses [20], and these lesions are often incidentally detected. The more data we can wring retrospectively from CTs obtained in the routine portal venous phase, without a special protocol, the more value we can add. Not only are we adding value to our CT studies, in some cases, we may be able to save the patient an additional imaging study. It is unlikely that techniques like this would supplant tissue sampling in the short term, but given that renal masses can be heterogeneous and biopsy may not fully capture the biologic behavior of the tumor, additional data may help support the biopsy result and can aid in treatment decisions at a time where more indolent lesions may be observed. In some cases, these decisions can be very complex, so a multimodality and multiparametric data model may be helpful. As above, if more direct radiologic-pathologic correlation can be performed, we could potentially use a technique like this to target biopsy in the future.

There were some limitations to our current study. The measurements were performed on small renal masses only. Groups have analyzed large renal masses (> 7 cm) but further study of intermediate-sized renal masses (4–7 cm) is warranted to gather a more complete picture of the relationship between texture and varying sizes of renal masses. In addition, given the small number of non-clear cell cases, aggressive tumors, and adverse outcomes in small renal masses, larger pooled or multi-center cohorts may have more utility in future studies. There was some heterogeneity in the CT technique used for the studies. It is not yet totally clear to what extent this impacts texture measures and what texture features are most robust and resistant to small differences in technique. It has been suggested that the filtration step may help emphasize biologic heterogeneity over image noise, but this requires further study. Finally, only a single slice of the tumor was sampled and volumetric assessment was not performed. There are, however, data suggesting that a single slice may be sufficient for this type of analysis [23, 31, 45]. Not all filter types were available for all masses, given the smaller size of the tumors included. The large number of predictors and filters used increases the risk of type I error, so it is possible that some findings of statistical significance may be spurious. However, a Bonferroni correction was applied during the statistical analysis to help minimize this. In addition, similar texture features that were identified in this study were similar to prior studies looking at RCC, supporting the idea that these associations are not spurious.

In summary, our results reveal that, for patients with small RCCs, CT texture features (in particular, entropy, SD of the pixel distribution histogram, and mean of the positive pixels) were associated with important histopathologic features. The textural differences detected may reflect the heterogeneous tumor microenvironment and the ability to provide useful clinical information such as predicting the presence of tissue biomarkers and protein expression has diagnostic and prognostic potential. As we gain more understanding of protein biomarkers and their clinical correlates, this information may be used in conjunction with other imaging features and clinical data to further risk stratify small RCC masses and to help select the most appropriate treatment (active surveillance, ablation, biopsy, resection) for these patients.

Compliance with ethical standards

Funding Funding support was provided by University of Wisconsin School of Medicine and Public Health Shapiro program and Department of Radiology Research and Development.

Disclosures MGL: Grant funding Philips, Ethicon. PJP: co-founder of VirtuoCTC, consultant for Bracco and Check-Cap, and shareholder in SHINE, Elucent, and Cellectar Biosciences. No other disclosures from the other authors

Ethical approval All procedures performed in studies involving human participants were in accordance with the ethical standards of the institutional and/or national research committee and with the 1964 Helsinki declaration and its later amendments or comparable ethical standards. The need for informed consent was waived.

References

1. Frank I, et al. (2003) Solid renal tumors: an analysis of pathological features related to tumor size. J Urol 170(6 Pt 1):2217–2220
2. Klatte T, et al. (2008) Tumor size does not predict risk of metastatic disease or prognosis of small renal cell carcinomas. J Urol 179(5):1719–1726

3. Pahernik S, et al. (2007) Small renal tumors: correlation of clinical and pathological features with tumor size. J Urol 178(2):414–417 ((**discussion 416-7**))
4. Young JR, et al. (2013) Clear cell renal cell carcinoma: discrimination from other renal cell carcinoma subtypes and oncocytoma at multiphasic multidetector CT. Radiology 267(2):444–453
5. Raman SP, et al. (2013) Chromophobe renal cell carcinoma: multiphase MDCT enhancement patterns and morphologic features. AJR Am J Roentgenol 201(6):1268–1276
6. Pierorazio PM, et al. (2013) Multiphasic enhancement patterns of small renal masses (</=4 cm) on preoperative computed tomography: utility for distinguishing subtypes of renal cell carcinoma, angiomyolipoma, and oncocytoma. Urology 81(6):1265–1271
7. Karlo CA, et al. (2014) Radiogenomics of clear cell renal cell carcinoma: associations between CT imaging features and mutations. Radiology 270(2):464–471
8. Egbert ND, et al. (2013) Differentiation of papillary renal cell carcinoma subtypes on CT and MRI. AJR Am J Roentgenol 201(2):347–355
9. Choi YA, et al. (2014) Subtype differentiation of renal cell carcinoma using diffusion-weighted and blood oxygenation level-dependent MRI. AJR Am J Roentgenol 203(1):W78–W84
10. Takeuchi M, et al. (2015) MRI for differentiation of renal cell carcinoma with sarcomatoid component from other renal tumor types. Abdom Imaging 40(1):112–119
11. Wang W, et al. (2014) Magnetic resonance imaging and computed tomography characteristics of renal cell carcinoma associated with Xp11.2 translocation/TFE3 gene fusion. PLoS ONE 9(6):e99990
12. Ganeshan B, Miles KA (2013) Quantifying tumour heterogeneity with CT. Cancer Imaging 13:140–149
13. Lubner MG, et al. (2017) CT texture analysis: definitions, applications, biologic correlates, and challenges. Radiographics 37(5):1483–1503
14. Ganeshan B, et al. (2012) Tumour heterogeneity in non-small cell lung carcinoma assessed by CT texture analysis: a potential marker of survival. Eur Radiol 22(4):796–802
15. Zhang H, et al. (2013) Locally advanced squamous cell carcinoma of the head and neck: CT texture and histogram analysis allow independent prediction of overall survival in patients treated with induction chemotherapy. Radiology 269(3):801–809
16. Yip C, et al. (2014) Primary esophageal cancer: heterogeneity as potential prognostic biomarker in patients treated with definitive chemotherapy and radiation therapy. Radiology 270(1):141–148
17. Ng F, et al. (2013) Assessment of primary colorectal cancer heterogeneity by using whole-tumor texture analysis: contrast-enhanced CT texture as a biomarker of 5-year survival. Radiology 266(1):177–184
18. Miles KA, et al. (2014) Multifunctional imaging signature for V-KI-RAS2 Kirsten rat sarcoma viral oncogene homolog (KRAS) mutations in colorectal cancer. J Nucl Med 55(3):386–391
19. Gandaglia G, et al. (2014) Contemporary incidence and mortality rates of kidney cancer in the United States. Can Urol Assoc J 8(7–8):247–252
20. Moreno CC, et al. (2016) Changing abdominal imaging utilization patterns: perspectives from medicare beneficiaries over two decades. J Am Coll Radiol 13(8):894–903
21. Raman SP, et al. (2014) CT texture analysis of renal masses: pilot study using random forest classification for prediction of pathology. Acad Radiol 21(12):1587–1596
22. Goh V, et al. (2011) Assessment of response to tyrosine kinase inhibitors in metastatic renal cell cancer: CT texture as a predictive biomarker. Radiology 261(1):165–171
23. Lubner MG, et al. (2016) CT textural analysis of large primary renal cell carcinomas: pretreatment tumor heterogeneity correlates with histologic findings and clinical outcomes. AJR Am J Roentgenol 207(1):96–105
24. Abel EJ, et al. (2014) Analysis and validation of tissue biomarkers for renal cell carcinoma using automated high-throughput evaluation of protein expression. Hum Pathol 45(5):1092–1099
25. Miles KA, et al. (2009) Colorectal cancer: texture analysis of portal phase hepatic CT images as a potential marker of survival. Radiology 250(2):444–452
26. Ganeshan B, et al. (2010) Texture analysis of non-small cell lung cancer on unenhanced computed tomography: initial evidence for a relationship with tumour glucose metabolism and stage. Cancer Imaging 10:137–143
27. Miles KA, Ganeshan B, Hayball MP (2013) CT texture analysis using the filtration-histogram method: what do the measurements mean? Cancer Imaging 13(3):400–406
28. Chow WH, et al. (1999) Rising incidence of renal cell cancer in the United States. JAMA 281(17):1628–1631
29. Stafford HS, et al. (2008) Racial/ethnic and gender disparities in renal cell carcinoma incidence and survival. J Urol 179(5):1704–1708
30. Nguyen MM, Gill IS, Ellison LM (2006) The evolving presentation of renal carcinoma in the United States: trends from the Surveillance, Epidemiology, and End Results program. J Urol 176(6 Pt 1):2397–2400 ((**discussion 2400**))
31. Ng F, et al. (2013) Assessment of tumor heterogeneity by CT texture analysis: can the largest cross-sectional area be used as an alternative to whole tumor analysis? Eur J Radiol 82(2):342–348
32. Nelson DA, et al. (2004) Hypoxia and defective apoptosis drive genomic instability and tumorigenesis. Genes Dev 18(17):2095–2107
33. Hodgdon T, et al. (2015) Can quantitative CT texture analysis be used to differentiate fat-poor renal angiomyolipoma from renal cell carcinoma on unenhanced CT images? Radiology 276(3):787–796
34. Ganeshan B, et al. (2013) Non-small cell lung cancer: histopathologic correlates for texture parameters at CT. Radiology 266(1):326–336
35. Eichelberg C, et al. (2009) Diagnostic and prognostic molecular markers for renal cell carcinoma: a critical appraisal of the current state of research and clinical applicability. Eur Urol 55(4):851–863
36. Wiesener MS, et al. (2001) Constitutive activation of hypoxia-inducible genes related to overexpression of hypoxia-inducible factor-1alpha in clear cell renal carcinomas. Cancer Res 61(13):5215–5222
37. Lidgren A, et al. (2005) The expression of hypoxia-inducible factor 1alpha is a favorable independent prognostic factor in renal cell carcinoma. Clin Cancer Res 11(3):1129–1135
38. Lidgren A, et al. (2006) Hypoxia-inducible factor 1alpha expression in renal cell carcinoma analyzed by tissue microarray. Eur Urol 50(6):1272–1277
39. Visapaa H, et al. (2003) Correlation of Ki-67 and gelsolin expression to clinical outcome in renal clear cell carcinoma. Urology 61(4):845–850
40. Gayed BA, et al. (2014) Ki67 is an independent predictor of oncological outcomes in patients with localized clear-cell renal cell carcinoma. BJU Int 113(4):668–673
41. Sandlund J, et al. (2006) Endoglin (CD105) expression in human renal cell carcinoma. BJU Int 97(4):706–710
42. Saroufim A, et al. (2014) Tumoral CD105 is a novel independent prognostic marker for prognosis in clear-cell renal cell carcinoma. Br J Cancer 110(7):1778–1784
43. Bauman TM, et al. (2016) Neovascularity as a prognostic marker in renal cell carcinoma. Hum Pathol 57:98–105
44. Sejima T, Miyagawa I (1999) Expression of bcl-2, p53 oncoprotein, and proliferating cell nuclear antigen in renal cell carcinoma. Eur Urol 35(3):242–248
45. Lubner MG, et al. (2015) CT textural analysis of hepatic metastatic colorectal cancer: pre-treatment tumor heterogeneity correlates with pathology and clinical outcomes. Abdom Imaging 40(7):2331–2337